JARTE
Journal of Applied Research in Technology & Engineering

5(1): 33-44, 2024
https://doi.org/10.4995/jarte.2024.20096
Received: July 23, 2023; Accepted: October 10, 2023; Published: January 31, 2024

SIMULATION-BASED POST-FAULT ANALYSIS IN WECS USING DFIG SYSTEMS UNDER AN UNBALANCED FAULT SCENARIO

Muzamil Hussain Wadho [a]*, Surat Khan [b], Sadqain Hassan [c], Muhammad Ahmed Kalwar [d]

[a] Electrical Engineering, BBSUTSD, Khaipur Mirs, Sindh, Pakistan.
[b] Department of Electrical Engineering BUITEMS, Quetta 87300, Pakistan.
[c] Department of Electrical Engineering, Quaid-e-Awam University of Engineering, Science & Technology Nawabshah, Sindh, Pakistan.
[d] Shafi Private Limited, Lahore, Pakistan.

[a] muzzamilhussein@bbsutsd.edu.pk, [b] surat.khan@buitms.edu.pk, [c] sadqainhassan08@gmail.com, [d] ahmedkalwar22@gmail.com

Abstract:

Fault analysis in an integrated Wind Energy Conversion System (WECS) is the highest priority factor to be taken into account for distributed generation (DG). The contribution of renewable energies (like solar and wind) to the power system is increasing continuously. New challenges are being faced while integrating such systems because of the no inertial response provided by renewable resources. So, for a reliable integration further exploration, development, and even new strategies are needed to improve the reliability, power quality, control and protection of renewable energy generation. Disintegration in distributed generation is still a huge question mark on the reliability of modern power systems. Disintegration has many causes and faults are one of them, that cause severe voltage profile distortions, which makes WECS a complex system in terms of control and protection of power system. In this work, focus has been paid to the analysis of asymmetrical faults in wind farms and their impacts are evaluated on the overall generation system. A 30 MW wind power plant has been developed in MATLAB to study the faults. Since wind farms are Low Voltage (LV) networks, therefore, fault impedance method (IEC 60909) and the Fort-cue Method have been used for the fault analysis. The fault current response and behaviour of the DG system under asymmetrical fault conditions at different locations in and around the wind farm have been obtained. It is found that fault loop impendence, transformer grounding type, and fault location largely affect the dynamic behaviour of the co-generation system under asymmetrical faults. In this work dynamic behaviour of the wind generation system has been analysed for the different asymmetrical faults induced at different locations of the system. The response of the wind generator has been evaluated based on the different fault simulations considering the sequence component method.

Keywords: wind energy; wind farm; fault analysis; disintegration.

Cite as: Wadho, M.H., Khan, S., Hassan, S., Kalwar, M.A. (2024). Simulation-based post-fault analysis in WECS using DFIG systems under an unbalanced fault scenario. *J Appl Res Technol Eng, 5*(1), 33-44. https://doi.org/10.4995/jarte.2024.20096

1. Introduction

The energy crisis and extreme carbonization in electricity production have become an alarming situation in Pakistan and the rest of the world. So in this regard, the graph of renewable energies is increasing every year. However, the massive penetration of renewable energies has raised power quality problems, control and stability issues and protection problems for modern power systems. Hence, deep learning is direly needed before connecting such renewable resources to the power grid. Solar and wind power generation have zero inertial response therefore when integrating these systems into the conventional grid, they produce disturbances in terms of operation, control, stability and protection of the giant grid. An example of this is the increase of the harmonic distortion at its point of Common Coupling (PCC) of the wind power Plant (WPP) with the power grid. Past studies have declared that major disturbance regarding wind farms and harmonics is associated with resonances when integrating with the local grid (Schwanz, 2019; Yang et al., 2014). Another cause of disturbance is the faults in and around the wind farms. The research subject here is fault disturbances and their effects on power systems. Wind farms consist of a conversion system, in which various types of generators are used, Type -3, Wound Rotor Induction Generator (also called Doubly Fed Induction Generator DFIG) is extensively used.

Type 3, Doubly fed induction generators (DFIG) with partial scale converters and type-4 Permeant Magnet Synchronous Generator (PMSG) with full-scale frequency convertors technologies are the most popular wind generators (Ackermann, 2005). PMSG technology is highly efficient and provides a robust connection to the grid through power electronics converters (Bradt et al., 2012; Liu et al., 2012). The equivalence model of DFIG is based on Norton's theorem.

Detailed mathematical modelling of DFIG is discussed in (Tapia et al., 2003), while relevant controlling schemes regarding fault ride-through are available in (Xie et al., 2013; Yang et al., 2012). An aggregate model of a wind farm with four 1.5 MW DFIGs (Doubly Fed Induction Generators) has been simulated. Results conclude that the dynamic

*Corresponding author: M.H. Wadho, muzzamilhussein@bbsutsd.edu.pk

behaviour of the simulated system using the Genetic Fuzzy controller is adequate under all types the faults except symmetrical faults. (Mahadanaarachchi, 2004). comprehensive study has been performed using different control strategies of LVRT (Low Voltage Ride Through) in DFIG wind turbine for the different fault conditions, this study reveals the effects of the above-mentioned faults at different levels (Peng et al., 2009). (Mahadanaarachchi, 2004) has carried out research on fault simulation for the protection of the system where only fault levels have been simulated. In this regard, a detailed study is needed which can provide and discuss the system-based causes of such faults so that faults can be optimized by providing suitable protection at proper locations inside such power systems.

This work focuses on the voltage profile and current-profile studies of the WPP under different fault scenarios and measurement of the fault currents so that the severity of faults is determined for the proper operation, control and protection of the system. It also focuses on the generators` behaviour under voltage imbalances due to different faults in WECS. It can help get the optimal location for protection system installation in WPP.

The first part of the paper discusses the introduction and the problem statement, second part consists of the mathematical model of the DFIG. In the third, fourth and fifth sections standard fault calculation methods, symmetrical component methods and fault contribution induction generators are discussed respectively. Finally, the Methodology is discussed in the sixth and the result discussion and conclusion are available in the seventh and eighth sections.

2. DFIG-Based WECS and its Fault Behaviour

2.1. Type C (DFIG- Variable-Speed Wind Turbine)

A power electronic converter has made a revolutionary concept of using variable-speed wind turbines with doubly fed induction generators as shown in Figure 1. In this system, the rotor of the generator is connected through a back-to-back (AC-DC-AC) converter, and the stator is connected to the grid directly. This type of WT is desirable for large power wind turbine systems because the power electronic converter consumes only 20-30 per cent of the cumulated power. It facilitates to design of the small-size converter, which results in, cost-effectiveness and low power losses.

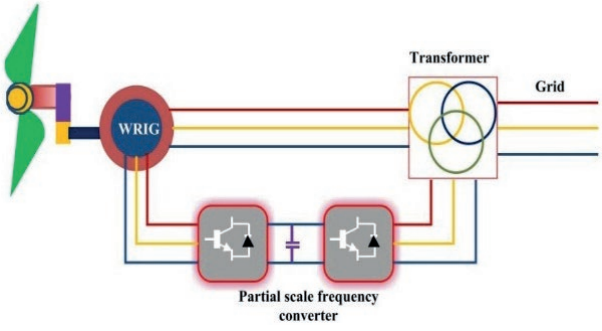

Figure 1: Variable Speed with DFIG (Type-C).

2.2. DFIG Modelling Aspects

Here induction machine modelling is discussed considering the two-phase (d-q) parameters. DFIG is a Wound Rotor Induction machine, that contains 3-phase stator winding, and the rotor contains slots in the outer periphery for housing the 3-phase winding. This machine can be represented by a transformer with a moving (secondary) rotor (Abbaszadeh et al., 2009).

2.3. D-Q Axis Modelling Approach of DFIG

The DFIG's modelling in the synchronously rotating frame can be done using d-q phases for the stator(ds-qs) and d-q phases for the rotor (dr-qr). The conversion of the three-phase quantities into two-phase quantities helps in reducing and simplifying the complex calculation of alternating quantities (You et al., 2012). The equivalent two-phase (d-q) diagram of the DFIG is shown in Figure 2.

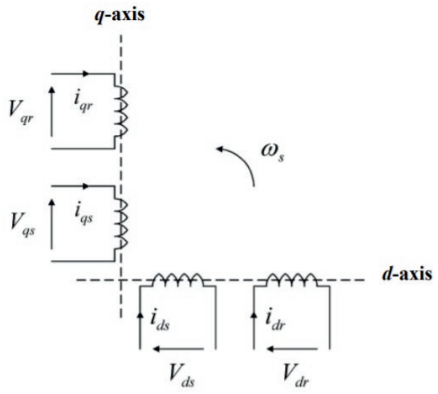

Figure 2: d and q axis representation of Stator and rotor winding (Peña et al., 2008).

The electrical equivalent circuit of DFIG is shown in Figure 3 and Figure 4.

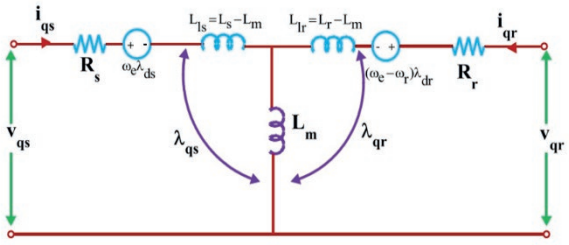

Figure 3: DFIG's two-phase equivalent circuit (q-axis circuit).

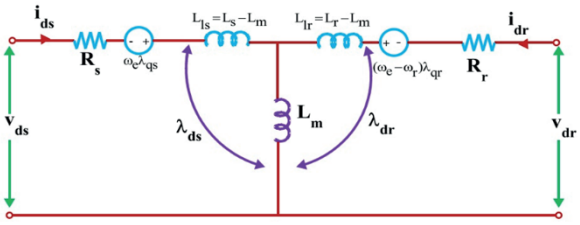

Figure 4: DFIG's two-phase equivalent circuit (d-axis circuit).

DFIG's three-phase stator and rotor voltages are given by the following expressions.

$$V_{abc(s)} = R_s i_{abc(s)} + \frac{d}{dt}\psi_{abc(s)} \quad (1)$$

$$V_{abc(r)} = R_r i_{abc(r)} + \frac{d}{dt}\psi_{abc(r)} \quad (2)$$

Using Park transformation, stator circuit equations for dq-phase are: (Peña et al., 2008)

$$V_{ds} = R_s i_{ds} + \frac{d}{dt}\psi_{ds} - (\omega_e \psi_{ds}) \quad (3)$$

$$V_{qs} = R_s i_{qs} + \frac{d}{dt}\psi_{qs} + (\omega_e \psi_{qs}) \quad (4)$$

Where ψ_{ds} and ψ_{qs} are the d & q axis flux-linkages respectively. Since all the terms are rotating at synchronous speed therefore bracketed terms show the back-emf. When ω_e is zero the back-emf becomes zero and d-q axis equations become stationary.

Similarly, the equations for the rotor, when the rotor is stationary or blocked i.e. ω_r=0, are given as

$$V_{dr} = R_r i_{dr} + \frac{d}{dt}\psi_{dr} - (\omega_e \psi_{dr}) \quad (5)$$

$$V_{qr} = R_r i_{qr} + \frac{d}{dt}\psi_{qr} + (\omega_e \psi_{qr}) \quad (6)$$

Here all the terms are referred to as the stator circuit (primary circuit). Suppose the rotor rotates at ω_r then the d-q axis of the rotor will rotate with a relative speed of $\omega_e - \omega_r$ now the rotor equations can be written as

$$V_{dr} = R_r i_{dr} + \frac{d}{dt}\psi_{dr} - (\omega_e - \omega_r)\psi_{dr} \quad (7)$$

$$V_{qr} = R_r i_{qr} + \frac{d}{dt}\psi_{qr} + (\omega_e - \omega_r)\psi_{qr} \quad (8)$$

Flux linkages in terms of the currents can be given as

Inductance = Flux linkage / Current (9)

Using the above expression, we have

$$\psi_{qs} = L_{qs} i_{qs} + L_m(i_{qs} + i_{qr}) \quad (10)$$

putting (i_{qs}=0) we get

$$\psi_{qs} = L_{qs} i_{qs} + L_m i_{qr} \quad (11)$$

$$\psi_{qs} = L_{qs} i_{qs} + L_m(i_{qs} + i_{qr}) \quad (12)$$

putting (i_{qr}=0) we get

$$\psi_{qr} = L_{qr} i_{qr} + L_m i_{qs} \quad (13)$$

For the d-axis

$$\psi_{ds} = L_{ds} i_{ds} + L_m(i_{ds} + i_{dr}) \quad (14)$$

$$\psi_{ds} = L_{ds} i_{ds} + L_m i_{dr} \quad (15)$$

$$\psi_{dr} = L_{dr} i_{dr} + L_m(i_{ds} + i_{dr}) \quad (16)$$

$$\psi_{dr} = L_{dr} i_{dr} + L_m i_{ds} \quad (17)$$

For the mutual flux linkages

$$\psi_{qm} = L_m(i_{qs} + i_{qr}) \quad (18)$$

$$\psi_{dm} = L_m(i_{qs} + i_{qr}) \quad (19)$$

The above are the basic equations that define the electrical behaviour of the DFIG. The model is based on the d-q transformation, consisting of stator and rotor windings on the direct axis and quadrature axis.

3. Standard Methods of Short-circuit Calculations

There are three standard methods of short-circuit current calculations (de Metz-Noblat et al., 2005).

3.1. Impedance Method

This method is a highly accurate method for fault current calculations. It involves the summation of resistances and reactance of the fault loop from the generator to the location of the fault. The symmetrical component method is useful for the fault current calculations of the three-phase unbalanced networks. Conventional "cyclical" Resistance (*R*) and reactance (*X*) are unusable.

The "impedance" method is a mathematical computational method. It is used for fault calculation at any point in an electrical power network with adequate accuracy. Finally, the short circuit current value is obtained using Ohm's Law.

$$I_{sc} = Vn / \sqrt{3}\sum(z) \quad (20)$$

Where I_{sc} represents short circuit current V_n network voltage and *z* is the total impedance of the system.

3.2. Composition Method

This method is well suited for the power supply network whose characteristics are unknown. The calculation of upstream impedance is made, based on the estimated fault current at its origin. *CosØ= R/X* for the network and fault location is assumed to be the same. For the accuracy in vector addition for the short circuit calculation, this assumption may be helpful.

3.3. Conventional Method

This method can be well suited for circuits whose impedances or short circuit currents are unknown. This method is useful for circuits having fault locations very far from the source. IEC 60909 (VDE 0102) with a voltage level of up to 550 kV can be put on a radial or meshed power supply system (de Metz-Noblat et al., 2005).

This technique calculates the equivalent voltage source at the fault area and calculates the fault current using Thevnin's theorem technique. All the sources and feeders of the network are replaced by the sequence impendence and capacitances and parallel admittances are neglected except, those for the zero-sequence system. Figure 5 depicts the sequence components.

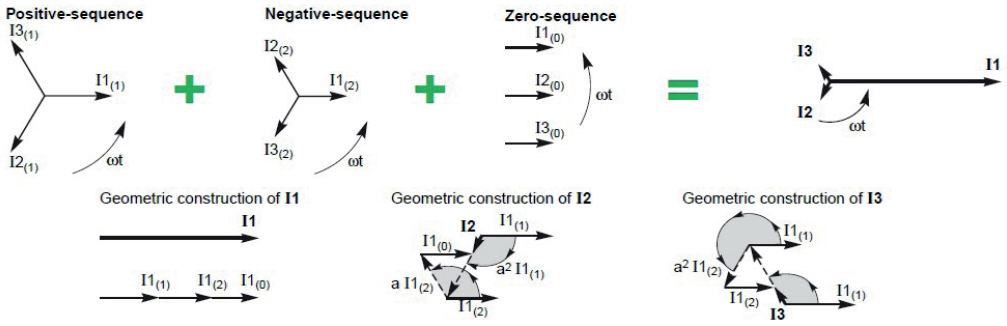

Figure 5: Positive negative and zero sequence components.

4. Symmetrical Component Approach and Its Benefits

Symmetrical components can be defined as an equivalence between asymmetrical 3Ø-system and the sum of 3Ø symmetrical system. Like Leblanc theorem, which states, "A rectilinear alternating sinusoidal field is equivalent to two rotating fields turning in the opposite direction". This method is required when imbalances in voltage and current exceed 120 degrees, like line-earth, line-to-line, and without ground connection.

5. Fault Contribution in Induction Generator

5.1. Fault Contribution of Induction Generator

Induction generators behave differently under fault conditions than synchronous generators do. This is because the process of induction provides the electromagnetic field in the air gap of the induction machine and separate field winding in such machines is not provided. Reactive power import, which is direly needed for maintaining the excitation of the Induction machine will be affected by the three-phase faults on the generator terminal (Lackey, 1951). As shown in Figure 6, fault current vanishes rapidly due to the fast decay of accumulated magnetic energy. Due to this reason, the fault current is limited to the sub-transient period only. The max: short circuit current of DFIG is given by (Tleis, 2019).

$$i_r(t) = \frac{\sqrt{2}\, V_{rms}}{(1-s)\sqrt{X^2} + R_{cb}^2}\left[e^{-\frac{t}{T_{cb}}} + e^{-t/T_a}\right] \quad (21)$$

Where T_a refers to the armature or stator time constant.

DFIG machine has the capability of operating at variable speeds from sub-synchronous and super-synchronous speeds. Thus slip of DFIG may deviate between s=0.3 (Sub-synchronous) and s=-0.2 (super synchronous) depending upon the design and rating of the machine. Therefore, the (1-s) in equation (21) cannot be unity in the case of DFIG. On the other hand, conventional asynchronous machines have slipped close to zero. Short circuit calculation and derivations are briefly explained in (Tleis, 2019). Inspection of equation (21) reveals that short circuit current varies inversely concerning the (1-s) that is if the machine initially runs at sub-synchronous rotational speed short circuit current amplitude is higher in initial cycles.

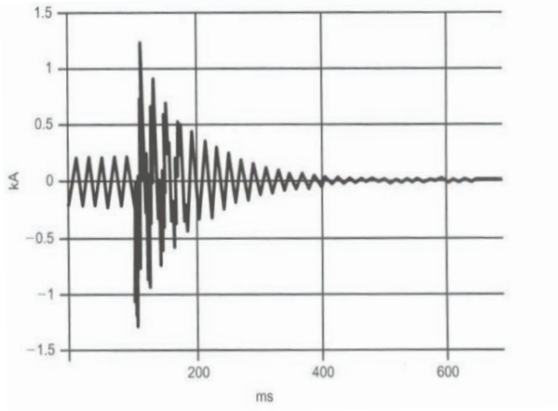

Figure 6: Short Circuit Current Characteristics of Induction Generator.

6. Research Methodology

6.1. Wind Farm Model

This research has been conducted, using real-time ratings of the 30MW wind farm of Sindh. This model consists of five wind turbines, each having a capacity of 4x1.5MW with a rated output voltage of 620V and 50Hz frequency. The wind turbines taken in this research are Doubly Fed Induction Generators (DFIG). The generator output is coupled to the pad-mounted Transformer, which steps up the low voltage of 620 V to a medium voltage level of 33 kV; it is located beside the tower base. All the medium voltages of the transformers are collected to a common bus called medium voltage bus or Collector bus (i.e. 33 kV bus). Medium voltage is further stepped up to a high voltage level of 132 kV with the help of the main transformer located in the substation, then this substation is linked to the grid at a point of common coupling (PCC). The model of the Plant is shown in Figure 7.

Parameters of the Wind turbine generator, Transformer, medium voltage, high voltage side, and underground cables.

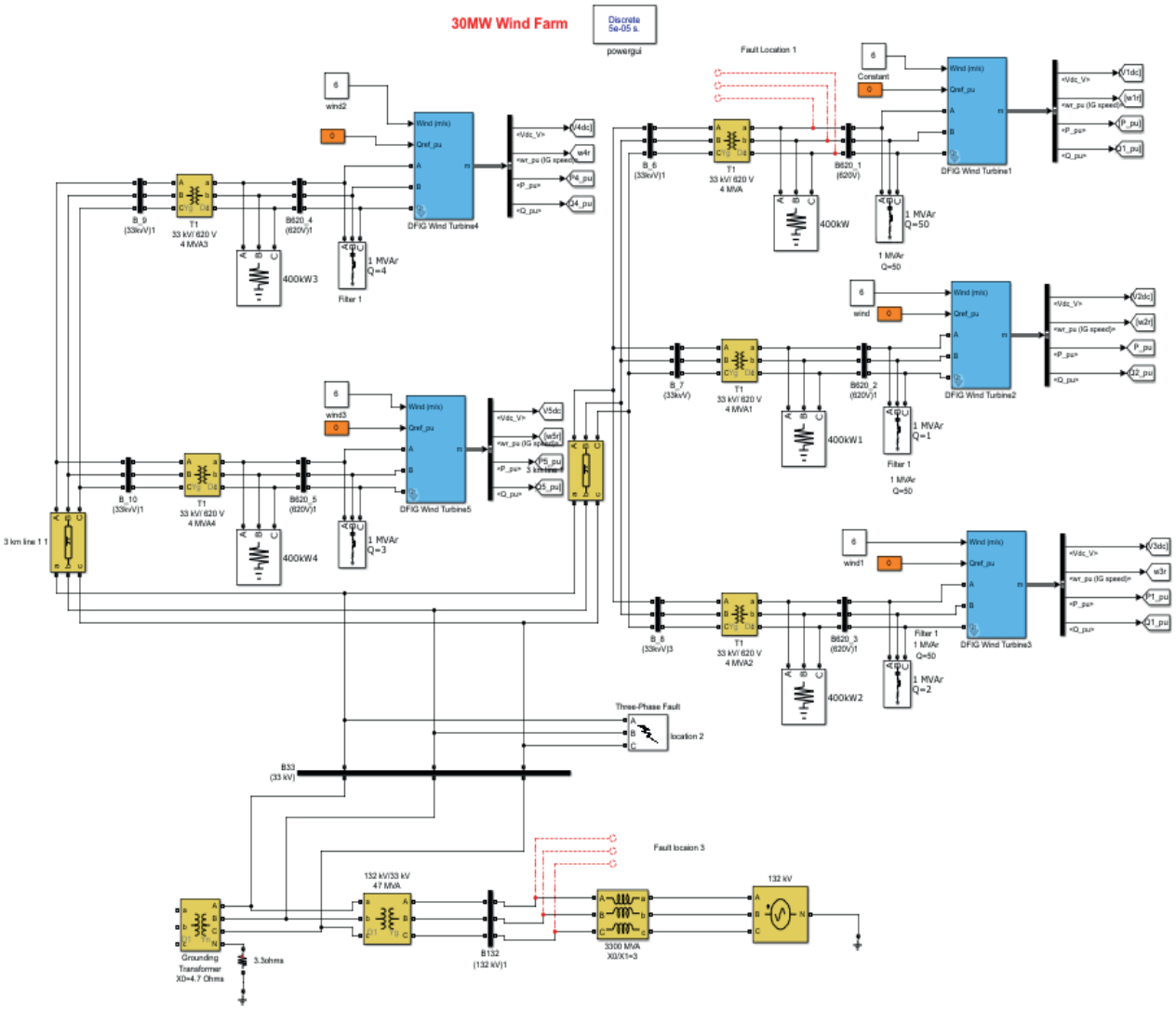

Figure 7: MATLAB model of the WECS.

6.2. Aggregated Model of Wind Farm in Matlab/ Simulink

Modelling of the wind farm has been done using MATLAB/ Simulink/Simpower system R2017a Library components.

Table 1: Equipment ratings and parameters of WECS.

S.no	Equipment/Parameters	Rating/value
1	Generator voltage	620 V
2	Generator power	1.5 MW
3	Frequency	50 Hz
4	Stator resistance	0.023 p.u
5	Stator inductance	0.18 p.u
6	Rotor Resistance	0.016 p.u
7	Rotor inductance	0.16
8	Collector Bus voltages	33 kV
9	High voltage transmission	132 kV
10	Wind speed	6 m/s

6.3. Simulation Procedure

In modelled wind farms symmetrical (three-phase short-circuited) faults and asymmetrical (L-G and L-L) faults have been introduced for analysis purposes at the three different locations. Locations are given below.

- Wind turbine generator
- 33 kV bus at the substation
- 132 kV transmission line

Time domain currents and voltages at Wind turbine generator-1 terminal, 33 kV bus in the substation bus were analysed for 1.5 s. Simulation starting time is taken as t=0, and switching time for the faults is taken as per the Gird code of National Transmission and Dispatch Company (NTDC) Pakistan is 0.1 s or 100 ms and 180 ms in case of circuit breaker stuck contingency (Wang et al., 2008). In this contrast, the fault switching time taken in simulation is t=0.3 s to t=0.4 s. A constant Fault resistance of 0.001 ohms has been taken. All the simulation results were achieved. Figure 8 shows the flow chart of the study

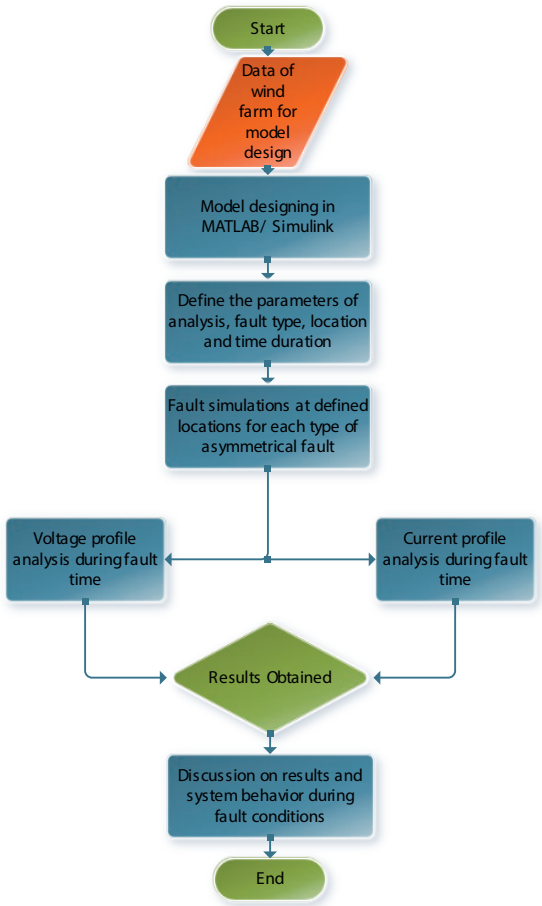

Figure 8: Research Methodology Diagram.

7. Results and Discussions

7.1. Unsymmetrical fault analysis of wind farms

There are the following types of Unsymmetrical or unbalanced faults analysed for the DFIG-based wind farms

- One Line-Ground fault (L-G)
- line-line fault (L-L)

7.1.1. L-G fault (Phase a - G) at 620v bus (Generator terminal)

Boundary conditions for L-G fault are:

$$Va = 0, \text{ and } Ib = Ic = 0$$

L-G (Line 'a' to Ground) fault is introduced on the wind turbine generator-1 terminal at t=0.3 s and cleared at 0.4 s. Voltages and currents in all three phases at the generator terminal are shown in Figure 9. Phase 'A' (Yellow) is grounded and the voltage in the faulted phase is zero. Normally WT is set to produce a voltage of up to 1 p.u. During the period of fault, the voltage in the other two phases 'B & C' (Red and Blue respectively) has increased approximately up to two p.u.

7.1.1.1. Voltage dip Analysis

This overshooting of the voltage in phases B and C depends upon the grounding of the Generator step-up Transformer. If it is not grounded or grounded through the resistor the voltage could be increased up to L-L values, but if it is solidly grounded then the voltages in the healthy phases will remain at L-G values.

On the other hand, there will also be some leakage capacitance in addition to the resistance to the ground. These are the causes of over-voltages in the other two non-faulty phases. Phase 'a' voltage drops to zero during the fault conditions. A small voltage drop has been observed in the other two non-faulty phases.

7.1.1.2. Current profile Analysis

For the current, it is clearly shown in the graph that during the initialization of the fault current in phase 'a', the fault current has increased up to 2.5 p. u which is 1.5 times greater than that of the current under normal conditions.

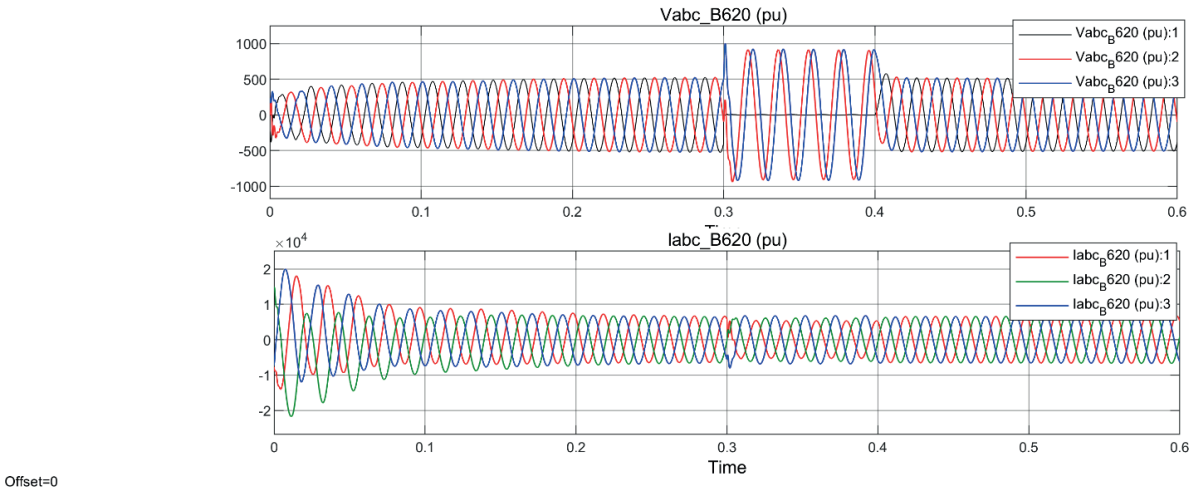

Figure 9: Voltage and current wave-forms at gen terminal.

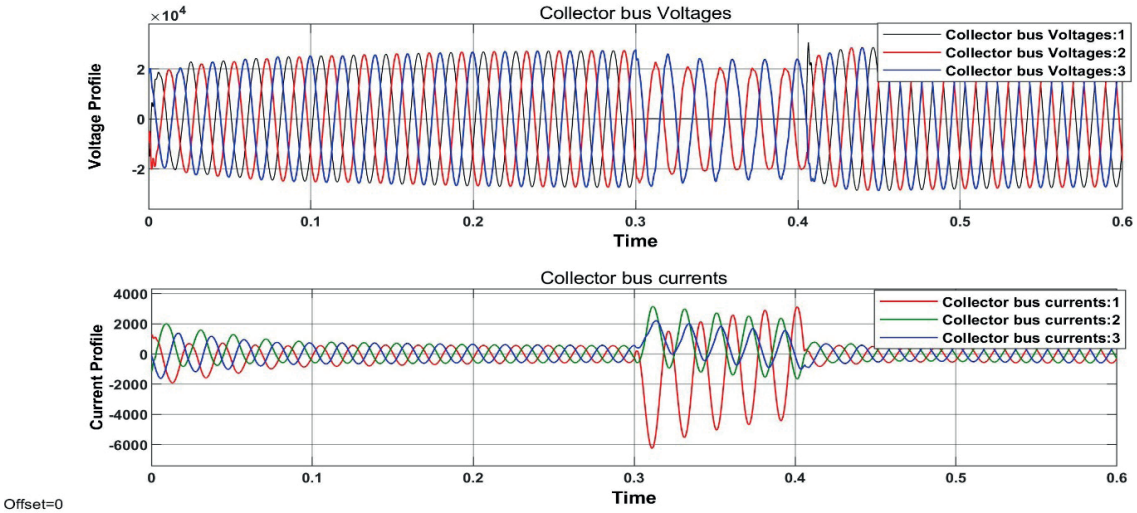

Figure 10: Fault at 33 kV bus.

The choke reactor connected to the generator panel limits the current. It indicates that without protecting the RSC (Rotor Side Convertor), the turbine cannot be operated in order to avoid damage to the power electronic converters during the fault condition.

7.1.2. L-G Fault at 33 kV Bus

L-G fault is introduced near the collector (33 kV) bus. The obtained voltage and current waveforms are shown in Figure 10. Phase 'a' voltage drops to zero during the fault conditions. A small voltage drop has been observed in the other two non-faulty phases.

7.1.2.1. Voltage Dip Analysis

This is because the collector bus zone of the wind farm is not grounded (fault location), and the fault current will travel towards the main transformer grounding. Since the distance between the fault location and the main Transformer grounding is considerably large (3 km in this study), the loop impendence of the zone also increases which causes a small voltage drop in the healthy phases. In the case of the generator the positive sequence impedance is greater than the negative sequence impedance, therefore during the fault time, fault current advances with a higher magnitude in the negative direction because of the low negative sequence impedance i.e. up to -8p.u. Since the positive sequence and zero sequence impedances are higher (But not infinite), therefore a small increase in the fault current is observed in two non-faulty phases.

Current waveforms for the L-G fault are shown in Figure 10. Current in Phase 'a' increases rapidly during the fault initialization and decays gradually. Since the collector, bus (33 kV) in the wind farms is not grounded. The effect of the L-G fault at the 33 kV bus is observed at the generator side as shown in Figure 11. During the fault, voltages in the yellow and blue phases at the generator-1 terminal are tone-downed but do not fall to zero. Analysis of the fault at the generator terminal during the fault at the 33 kV bus shows that voltages are dropped in the yellow and blue phases with approximately

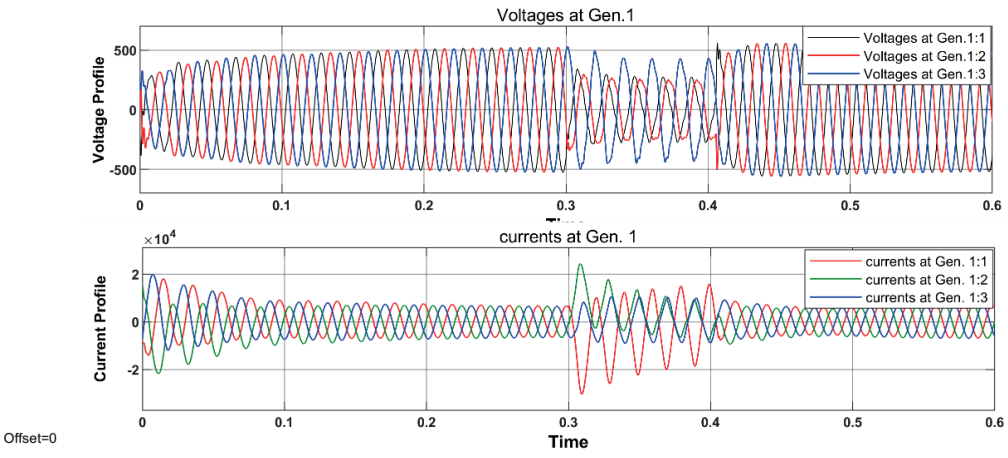

Figure 11: Voltage and current waveforms at generator terminal for L-G fault at 33 kV Bus.

equal amounts. Since 33 kV, the collector zone is not grounded therefore fault current flows towards the generator transformer grounding. Therefore, a drop in the phases is recognized by the sequence impendance characteristics of the transformer and the fault loop impedance between the point of fault and grounding of the transformer. In the case of the transformer the positive sequence, impedance is equal to the negative sequence impedance, therefore during the fault time, fault current advances with approximately the same magnitude in the negative and positive direction in the yellow phase and blue phase respectively. Another cause behind this situation is the presence of residual voltages caused by the line capacitance and fault loop impedance provided by the step-up transformer connected between the Generator and the 33 kV bus.

7.1.3. L-G Fault at 132 KV Line

For the L-G fault near the high voltage transmission line (132 kV), the obtained current and voltage waveforms are shown in Figure 11, which is given as under. L-G fault is introduced near high voltage bus. The voltage in the faulty phase 'a' exactly drops to zero. While the other two phases experience a small voltage, overshoot of approximately 0.25 p.u.

The maximum current produced by the generator is 2 p.u since the fault current is about 8 p.u. The phrase 'a' current of the High voltage transmission line is much greater than that of the wind plant side during the fault time. Since the wind power plant is a weak supply system as compared to the grid, the short circuit current provided by the wind farm is smaller than that of the grid side. The fault current travels in both directions i.e. towards the grid and wind farm. On both sides, transformers are installed and fault current will complete its path through the grounding of the transformer. In this situation, zero sequence currents are dominant, and positive and negative sequence currents are absent, hence the deviation in the 3-φ currents is not obvious and all the phase currents are in phase with each other as shown in Figure 12. A large amount of the current in all three phases is produced. Such type of large currents can saturate the C. Ts and PTs and can be the cause of the failure of the protection system in wind power plants.

7.2. Unsymmetrical Faults (L-L)

7.2.1. 1 L-L Fault (Line b - c) at generator terminal

Line-Line fault (Phase B and Phase C) is created on the Wind turbine generator-1 terminal at the time of 60ms. Voltage and current in all the phases obtained at 620 V bus-1 Generator terminal are shown in given below Figure 13. During the initialization of fault, the voltages in the phases b and c are considerably town down that is Vb = Vc, and the Voltage overshoot in the non-faulty phase is observed, which completely matches with the theoretical results.

As per theoretical results, current in the phase 'b' should go through the current in phase 'c' in an equal amount but opposite in direction. I.e. Ib = -Ic. The analysed results of the simulation clearly show that the current in Phase B and Phase C are equal but opposite in direction during the fault period. Ideally, current in the phase 'a' should decay to zero, but in this case, the presence of the current in phase 'a' is due to the current fed from the other generators of the wind farm and power system.

7.2.2. Fault (Phase b - c) at 33 kV Bus

7.2.2.1. Effect observation at Generation Terminal

L-L fault is introduced at 33 kV bus for the time of 60ms. The voltage and currents for the fault are shown in Figure 14. At the time of initialization of fault, the voltage dips are observed in phase 'b' and 'c', the phenomenon is in line with the theoretical conditions. The current in the faulty phases 'b' and 'c' are equal and opposite which is totally in phase with the theoretical result. The current in phase 'a' should theoretically decay to zero, but here in phase 'a' small transient current during the fault period is observed because the fault current is also fed by the other generators of the wind farms.

7.2.3. L-L Fault at 33 kV Bus Itself

L-L fault is introduced near the collector bus (33 kV). Observed voltages and currents are shown in Figure 15, which is given as under.

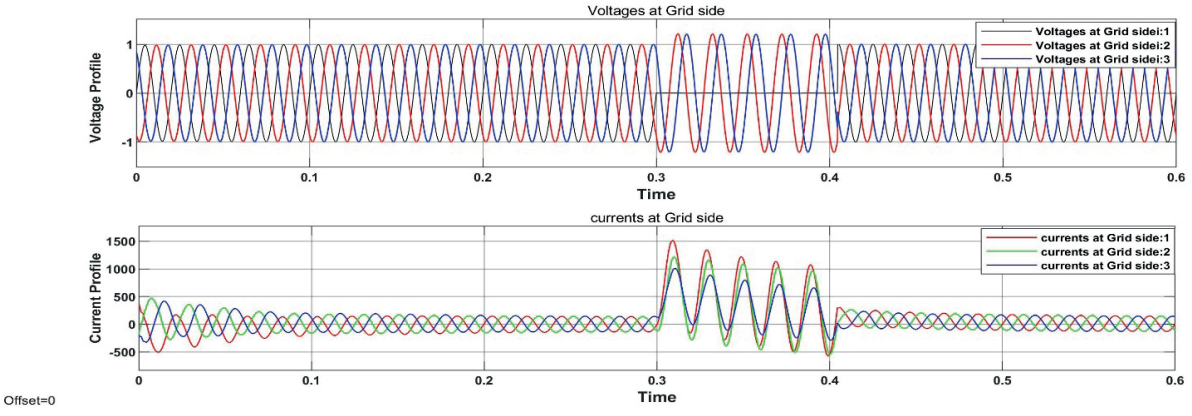

Figure 12: L-G at 132 kV bus.

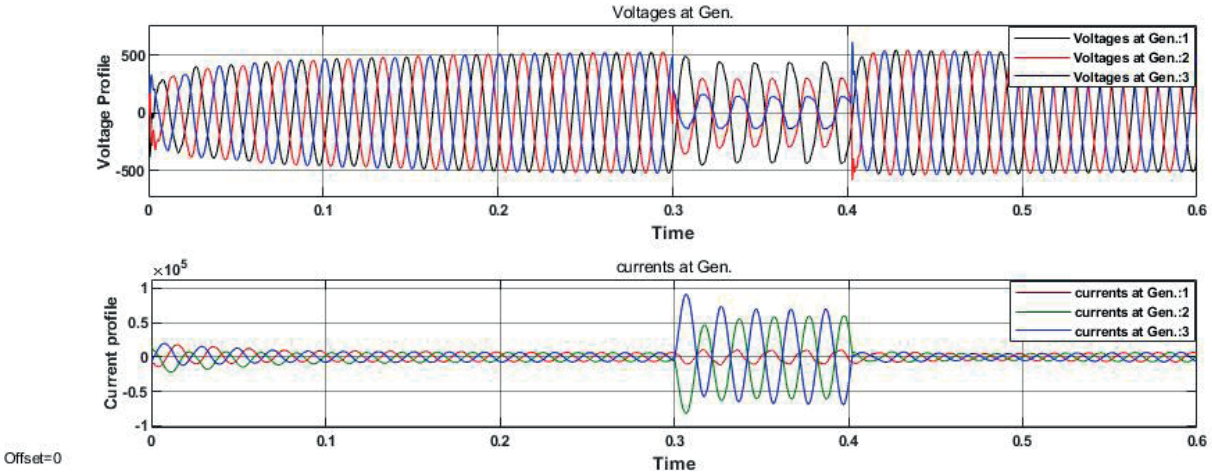

Figure 13: L-L fault (Phase b - c) at generator terminal.

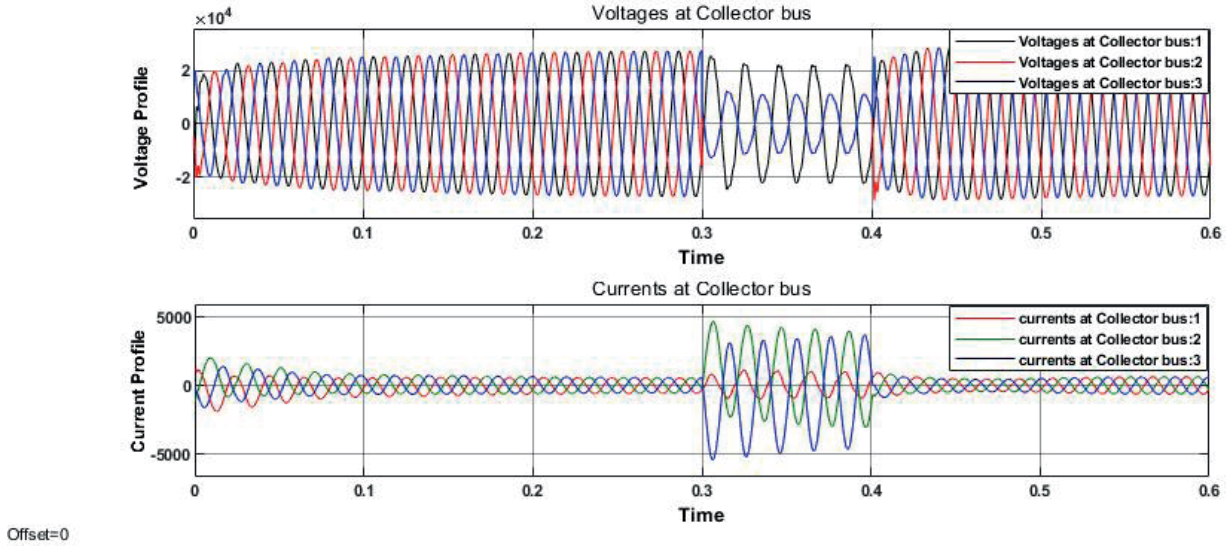

Figure 14: L-L fault (Phase b - c) at 33 kV Bus.

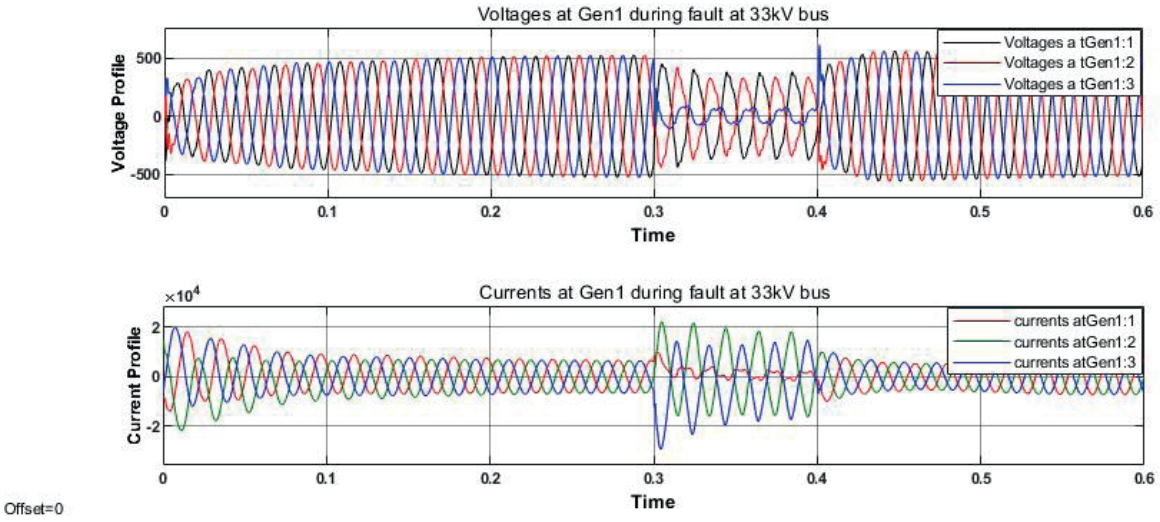

Figure 15: L-L fault (Phase a - b) at 33 kV bus observed voltage and currents at gen: terminal.

Figure 15 shows that the fault on the 33 kV bus directly affects the terminal voltages of the generators. Considerable decreases in the voltages of all phases can be seen. Moreover, large severe currents are flowing during fault time. In this condition, the generator will consume more reactive power from the grid to maintain its terminal voltages but if the fault lasts for a longer time it will lead the system towards cascading failures.

Results obtained for the L-G asymmetrical faults are given in Table 2, and L-L faults results are given in Table 3.

Table 2: Asymmetrical Line –Ground (L-G) fault.

Line –Ground Fault	Max: short circuit current in p.u	Voltage in p.u Column
1. At Gen: Terminal	3p.u	Phase-a= 0 Phase- b-c=1.8p.u
2. 33 kV Collector Bus	-8p.u to 4p.u	Phase-a= 0 Phase-b=0.7p. u Phase-c= 0.9p.u
3. 132 kV Transmission Line	8p.u to 3p.u	Phase-a= 0 Phase b=c= 1.5 p.u

Table 3: Line-to-line fault.

Line –Line Fault	Max: short circuit current in p.u	Voltage in p.u Column
1. At Gen: Terminal	10 p.u to -10 p.u	Phase-a= 0 Phase- b-c=1.8 p.u
2. 33 kV Collector Bus	-7 p.m. to 6 p.u	Phase- a=1.5 Phase-b=c=0.2

8. Findings

This work explores the transient behaviour of the WECS during the faults through the graphical representation of each fault. Each of the simulation results is justified by the different possible factors.

- Grounding of the step-up transformer in the fault analysis affects the fault behaviour, such as overshoot of the voltages in the healthy phases observed.
- It is found that negative sequence currents are produced during the asymmetrical faults, which invert the phase sequence of the system hence, can cause the loss of synchronism with the grid and protection coordination can be affected at large.
- The effect of the fault loop impedance is observed, and the influence of the sequence impedances of the generator, transformer, and transmission line on the behaviour of faults has been discussed.
- Power oscillations are observed (Which are unacceptable by the grid codes).

8.1. Consequences of Faults on Power System

8.1.1. Effects of Grounding Methods

It is found that Grounding methods are major causes of the overvoltage in healthy phases during the fault conditions. If the primary of the Transformer is ungrounded or grounded through resistor L-G voltages on unfaulty phases approaches to line-line values.

8.1.2. Effects of Voltage swells

- This can cause severe damage to single-phase loads.
- Insulation damage can occur due to over-voltages of expensive equipment.
- The transformer can be saturated and damaged.
- Insulators and lightning arrestors will flash over and breaker bushing may fail.

8.1.3. Effects of Voltage Dips

- High rotor currents are produced which causes the DC link voltage to rise (Which is undesirable)
- Voltage dips at GSC cause poor power feeding to the grid.

8.1.4. Effects of Power Oscillation

- At the instant of fault start and fault clearance power oscillations are produced in the rotor and stator circuit.
- Variable power input to the grid is not acceptable to the grid codes.
- If these oscillations continuously increase, it can cause the generator to lose stability.
- Due to voltage, dips during the fault high rotor currents are produced which causes the rotor speed to increase.

8.2. Effects on the Protection Coordination

Faults sources in DG system

- Distributed Generation side only
- Grid side only
- Both

In this situation protection coordination issue are raised, that affects the operating time of the relying system, sensing of the reverse faults, and so on. Transients of different faults are obtained with maximum short circuit values in p.u that could help in the effective selection of instrument transformers switchgear etc. for the wind farm protection.

9. Conclusion

In this research work, the dynamic behaviour of the wind farms equipped with DFIGs is studied, under the asymmetrical fault conditions at three different locations inside and outside the wind farms. It shows that when a line-ground fault occurs, at the generator terminal the magnitude of the fault current is adequate to be eliminated by the Crowbar protection of the DFIG. Because the fault current has, a lower magnitude and fault loop impedance is low, the fault current can flow towards the grounding of the pad transformer which is located near DFIG. For a similar fault, if it occurs on the grid side, it is found that very heavy currents in all three phases are present along with the zero-phase

sequence components. In addition, the effect of the fault loop impedance, and the influence of the sequence impedances of the generator, transformer, and transmission line are discussed to elaborate on the behaviour of faults. It is also found that asymmetrical faults at 33 kV bus and near points of common coupling largely affect the operation of wind generators. As L-L fault at 33 kV bus produces a severe imbalance in the magnitude and phase sequence is reversed in two phases, while in one phase multiple frequency components have also been observed as well. The fault analysis information facilitates grid operators in designing an effective control coordination in managing grid stability. This work is helpful for developing strong protection coordination for the smooth operation of the power system with an optimal fault location. It can also help in understanding the cascading and islanding conditions of such systems that cause disturbance in co-generation systems. In contrast to [9], where only levels of faults have been obtained and discussed for updating the grading of the system, this work focuses on the effects of faults on the behaviour of the wind generators.

References

Abbaszadeh, A., Lesan, S., & Mortezapour, V. (2009). Transient response of doubly fed induction generator under voltage sag using an accurate model. *1st IEEE-PES/IAS Conference on Sustainable Alternative Energy, SAE 2009 - Proceedings*, 1–6. https://doi.org/10.1109/SAE.2009.5534834

Ackermann, T. (2005). Wind Power in Power Systems. In *Wind Power in Power Systems*. John Wiley & Sons, Ltd. https://doi.org/10.1002/0470012684

Bradt, M., Badrzadeh, B., Camm, E., Mueller, D., Schoene, J., Siebert, T., Smith, T., Starke, M., & Walling, R. (2012). Harmonics and resonance issues in wind power plants. *Proceedings of the IEEE Power Engineering Society Transmission and Distribution Conference*. https://doi.org/10.1109/TDC.2012.6281633

Lackey, C.H.W. (1951). *Fault Calculations: The Calculation of Currents and Voltages Resulting from Faults in Electrical Power-systems* (reprint). Oliver & Boyd.

Liu, S.Y., Pimenta, C.M., Pereira, H.A., Mendes, V.F., Mendonca, G.A., & Silva, S.R. (2012). Aggregated inverters wind farm harmonic propagation analysis c. *Proc. XIX Congresso Brasileiro de Automática*, 1–8. https://doi.org/10.13140/2.1.3148.0326

Mahadanaarachchi, V.P. (2004). *Fault analysis and protection of doubly fed induction generator-based wind farms* [University of Moratuwa]. https://shareok.org/handle/11244/10239

de Metz-Noblat, B., Dumas, F., & Poulain, C. (2005). Calculation of short-circuit currents. *Cahier technique 158*.

Peña, R., Cárdenas, R., Proboste, J., Asher, G., & Clare, J. (2008). Sensorless control of doubly-fed induction generators using a rotor-current-based MRAS observer. *IEEE Transactions on Industrial Electronics*, *55*(1), 330–339. https://doi.org/10.1109/TIE.2007.896299

Peng, L., Francois, B., & Li, Y. (2009). Improved crowbar control strategy of DFIG based wind turbines for grid fault ride-Through. *Conference Proceedings - IEEE Applied Power Electronics Conference and Exposition - APEC*, 1932–1938. https://doi.org/10.1109/APEC.2009.4802937

Schwanz, D. (2019). *On Transfer Functions for Power Quality Studies in Wind Power and Solar PV Plants* [Lulea University of Technology]. https://www.diva-portal.org/smash/get/diva2:1266963/FULLTEXT01.pdf

Tapia, A., Tapia, G., Xabier Ostolaza, J., & Sáenz, J.R. (2003). Modeling and control of a wind turbine driven doubly fed induction generator. *IEEE Transactions on Energy Conversion*, *18*(2), 194–204. https://doi.org/10.1109/TEC.2003.811727

Tleis, N. (2019). Power systems modelling and fault analysis: Theory and practice. In *Power Systems Modelling and Fault Analysis: Theory and Practice*. Elsevier. https://doi.org/10.1016/C2017-0-02262-0

Wang, W., Pan, Z.C., Cong, W., Yu, C.G., & Gu, F. (2008). Impact of distributed generation on relay protection and its improved measures. *2008 China International Conference on Electricity Distribution, CICED 2008*. https://doi.org/10.1109/CICED.2008.5211797

Xie, D., Xu, Z., Yang, L., Ostergaard, J., Xue, Y., & Wong, K.P. (2013). A Comprehensive LVRT Control Strategy for DFIG Wind Turbines with Enhanced Reactive Power Support. *IEEE Transactions on Power Systems*, *28*(3), 3302–3310. https://doi.org/10.1109/TPWRS.2013.2240707

Yang, L., Xu, Z., Østergaard, J., Dong, Z.Y., & Wong, K.P. (2012). Advanced control strategy of DFIG wind turbines for power system fault ride through. *IEEE Transactions on Power Systems*, *27*(2), 713–722. https://doi.org/10.1109/TPWRS.2011.2174387

Yang, K., Bollen, M.H.J., Larsson, E.O.A., & Wahlberg, M. (2014). A statistic study of harmonics and interharmonics at a modern wind-turbine. *Proceedings of International Conference on Harmonics and Quality of Power, ICHQP*, 718–722. https://doi.org/10.1109/ICHQP.2014.6842921

You, Y.M., Lipo, T.A., & Kwon, B.I. (2012). Optimal design of a grid-connected-to-rotor type doubly fed induction generator for wind turbine systems. *IEEE Transactions on Magnetics*, *48*(11), 3124–3127. https://doi.org/10.1109/TMAG.2012.2200667